Draft version September 15, 2022
Typeset using LaTeX/show your work! modern style in AASTeX631

The imprint of global magma oceans on exoplanet demographics

Martin Schlecker [1] and al.

[1] *Department of Astronomy/Steward Observatory, The University of Arizona, 933 North Cherry Avenue, Tucson, AZ 85721, USA*

ABSTRACT

... magma oceans ...

Here, we assess the ability of space and ground-based telescopes to test this hypothesis using Bioverse, a simulation framework that leverages contextual information from the overall planet population. ...

1. INTRODUCTION

papers: ???. (?, water loss, O2 buildup around M dwarfs),

Several patterns in the planetary parameter space have been reported in demographic studies or predicted from planet formation theories. ...long-term goal/overarching objective: derive the geophysical history of rocky extrasolar planets. More concrete: Constrain the limits of runaway greenhouse transitions, and thus the inner edges of the habitable zone. Also: How close is Earth from this runaway greenhouse limit?

...

introduce magma oceans and their influence on planetary radii (Dorn & Lichtenberg 2021).

...current/future observations of planets that are currently in the runaway greenhouse phase may constrain properties of their planetary mantles... make connection between interior and atmospheres.

2. GLOBAL MAGMA OCEANS AND THEIR IMPRINT ON EXOPLANET DEMOGRAPHICS

"Methods Section" for the geophysical models.

Main assumptions:
- Assume that every planet has *some* water. Enough for runaway GH under the right conditions. Baseline water content: 20%
- Limitation to small planets without significant atmospheric envelopes.
- we ignore water loss by H_2O photolysis in the upper atmosphere and subsequent H escape, which would eventually cool even planets within the runaway greenhouse regime (Lichtenberg et al. 2022).
- we ignore tidal heating, which could extend the magma ocean phase of close-in planets (and change their orbits via tidal orbital evolution)(Jackson et al., 2008; Barnes et al., 2013 (?)).

2.1. *Global magma oceans*

introduce geophysical model.
Introduce its parametrization either here or further down when modeling demographic imprint.
Figure 2 goes here.

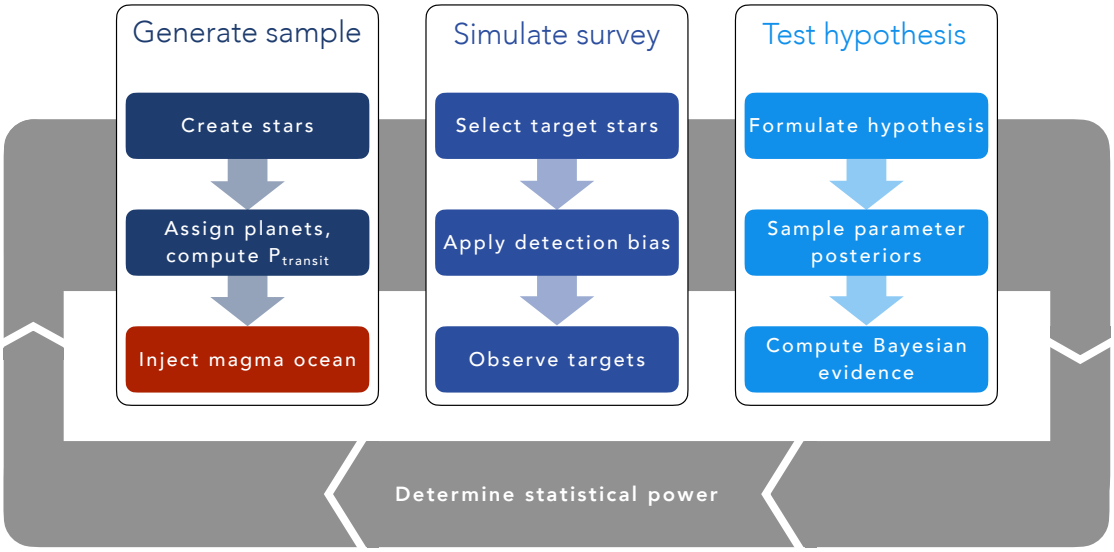

Figure 1. Workflow of our hypothesis testing with Bioverse. In the first block, a stellar sample is generated based on XXX. The stars are then populated with planets from XXX, which may be assigned a magma ocean based on the model described in Sect. 2.2.1. The planets' respective transit probabilities are computed. The second block simulates the exoplanet survey whereby selection effects and detection biases are introduced. Finally, the third block deals with testing a hypothesis based on the data from the simulated survey. By iterating through these steps, we compute the statistical power of testing the hypothesis given the assumed survey design.

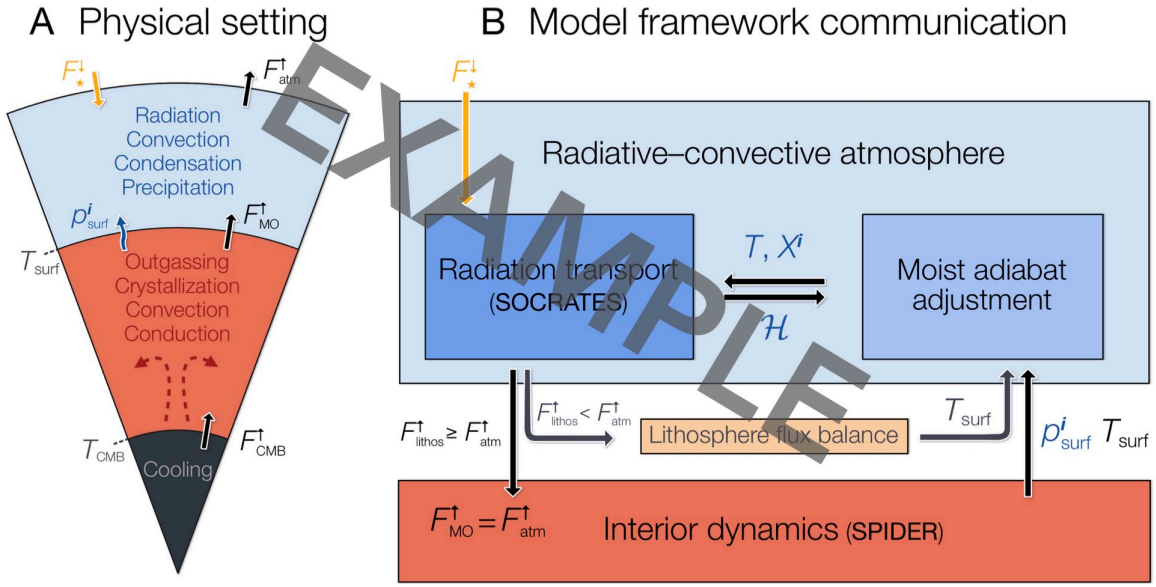

Figure 2. Schematics of the geophysical model framework.

2.2. *Demographic imprint of magma oceans*

describe the expected imprint on the exoplanet population.
Provide parametrizations from Dorn & Lichtenberg (2021)'s models.

2.2.1. *Parametrization*

specific parametrization, dependency on bulk planet/orbit params (doesn't have to be its own subsubsection)

The power from the host star per unit area at the position of a planet or stellar insolation S in units of Earth's insolation is given by

$$\frac{S}{S_\oplus} = \left(\frac{L_\star}{L_\odot}\right)\left(\frac{au}{a}\right)^2. \tag{1}$$

We further define the solar-equivalent semi-major axis $a_{eff} = a(L_\star/L_\odot)^{-1/2}$, at which a planet experiences the same insolation as a Solar System planet at an orbital distance a.

3. TESTING THE MAGMA OCEAN HYPOTHESIS

"Methods Section" of the hypothesis testing part. Introduce the idea of constraining magma ocean frequencies and/or physics with Bayesian stats on exoplanet population; introduce Bioverse; report methods of the hypothesis tests.

3.1. *Synthetic star and planet sample*

The first step in our analysis is to generate a synthetic sample of stars and planets. First, we create a stellar population based on the observed population in the solar neighborhood, to which we then assign planetary systems based on occurrence rates derived from the *Kepler*mission. In our fiducial model setup, we consider stars with a maximum distance to the solar system of $50\,\mathrm{pc}$.

3.1.1. *Stellar sample from Gaia DR3*

Which star sample was actually used?

3.1.2. *Planetary ocurrence rates in orbital period and radius*

What is the source of our occurrence rate density from which we draw? We could also use a generative model that directly approximates an observed or theoretical density (e.g., Schlecker et al. 2021).

The NASA Exoplanet Program Analysis Group chartered Science Analysis Group 13 (SAG 13)... The inferred occurrence rate density can be expressed as a power law in planet radius and period

$$\frac{\partial^2 n}{\partial \log R\, \partial \log P} = \Gamma R^\alpha P^\beta \tag{2}$$

that is broken in planet radius, resulting in the free parameters Γ, α, β, and a breakpoint radius R_{break}.

3.1.3. *Stellar luminosity tracks*

if implemented, describe the luminosity evolution of stars

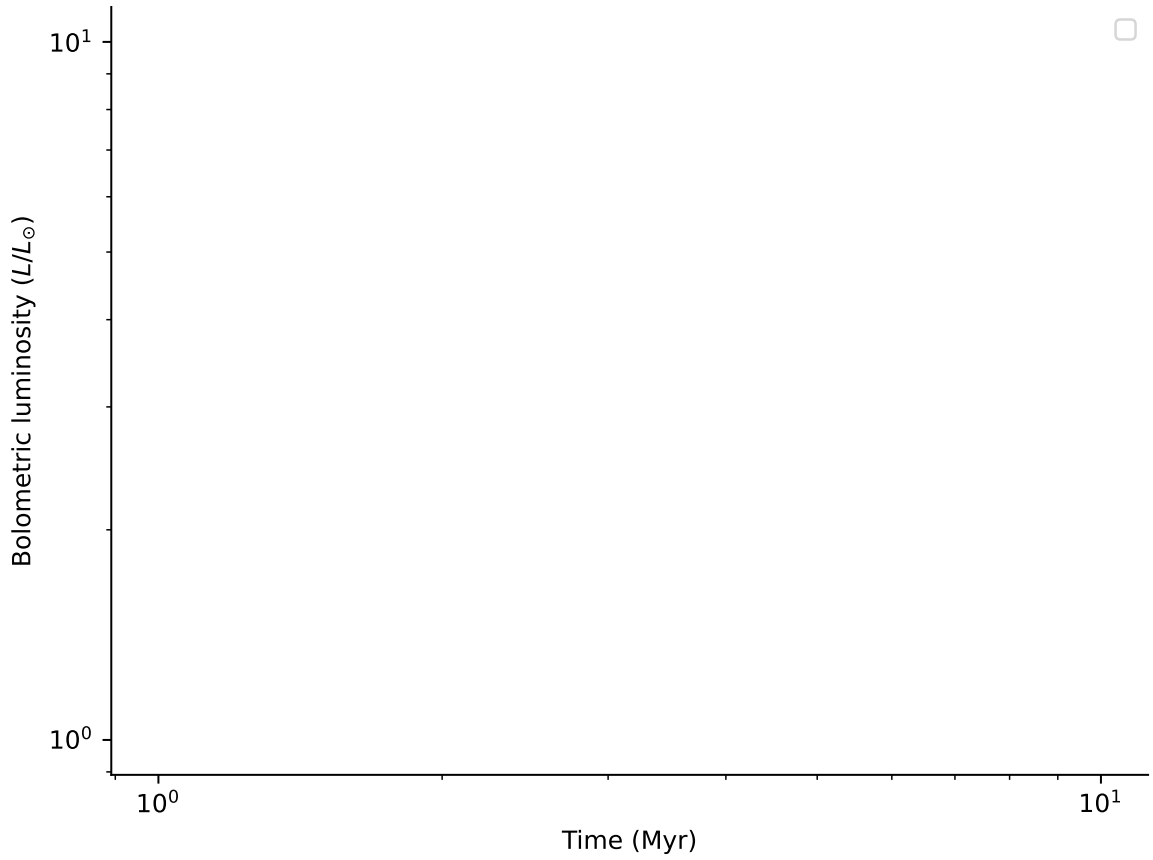

Figure 3. Bolometric luminosity tracks of stars with different masses.

3.1.4. *Transit probability*

describe how we model inclinations and transits of synthetic planets

Not all planets are transiting from our point of view. We model the occurrence of transits by assuming random, isotropic orientations of planetary orbits and calculating the transit impact parameter $b = \cos(i)/R_\star$ for each planet. Only planets with $|b| < 1$ are transiting and further considered. For these cases we calculate the transit depth

$$\delta = \left(\frac{R_\mathrm{P}}{R_\star}\right)^2 \tag{3}$$

check if transit depth or duration are actually used further down

and transit duration

$$t_\mathrm{T} = \frac{R_\star P}{\pi a}\sqrt{1-b^2}, \tag{4}$$

which are relevant for the detection probability of the respective planet (see Sect. ??). After excluding all non-transiting planets, the size of our nominal sample of potentially observable planets drops to $N = 733$.

3.1.5. *Synthetic planet populations with and without magma oceans*

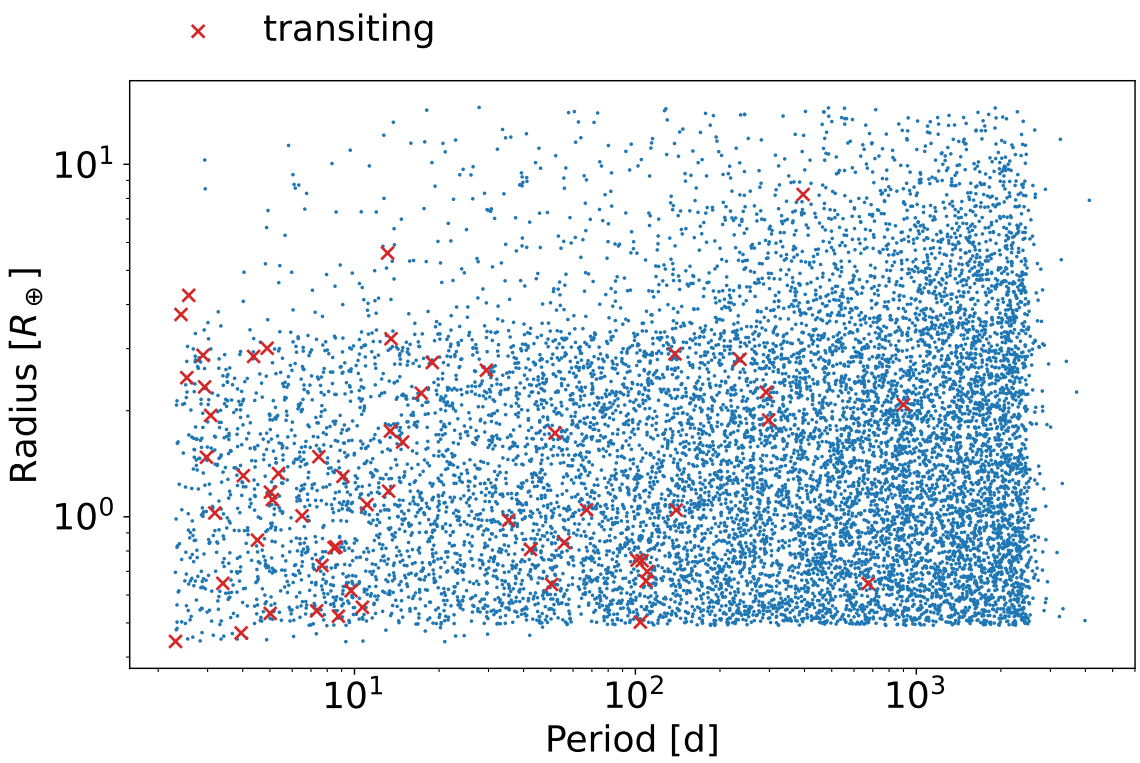

Figure 4. Total synthetic planet population and transiting planets.

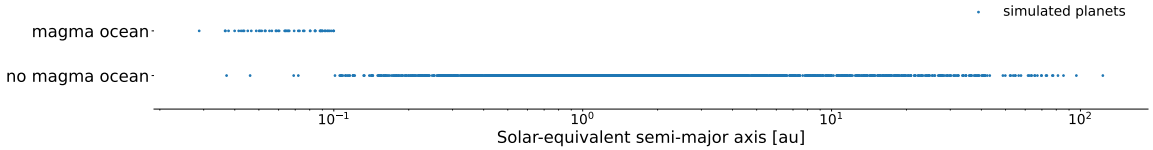

Figure 5. Synthetic planets with and without magmaoceans as a function of Solar-equivalent semi-major axis

describe the way we inject magma oceans into the synthetic planet population with Bioverse

Transition to tests of the trend:

Figure 5 shows that the subpopulation of planets with magma oceans is apparent in the synthetic dataset. In the following, we test if and under what conditions this effect is large enough to be detected with high significance.

3.2. *Testing the magma ocean hypothesis with current and planned exoplanet missions*

Introduce survey simulation(s). PLATO, Cheops, Ariel, LIFE?, Nautilus
What are threshold missions that are able to detect this signal? =>X meter working for Y years, or X' meter working for Y' years
=> conclusion could be that there is interesting science to do with intermediate size telescope.

In previous steps, we generated a population of synthetic planets that orbit synthetic stars, and we have injected the statistical trend expected from the presence of magma oceans on a fraction of the planets. Only a subset of these planets would be detectable by a transit survey, and their properties can be probed only with a finite precision. To test

the detectability of a magma ocean signature, we simulated several transit surveys with different designs and strategies and explored their capability to recover the magma ocean trend and constrain its parameters. We assessed this capability based on two determinants: the likelihood that the mission is able to detect the injected trend, and the precision with which it can constrain the parameters of that trend. ...

We consider a number of key parameters of transit surveys: The telescope's mirror diameter (or effective diameter for a telescope array) D, the total time budget of the survey for observations $t_{\rm total}$, the maximum number of observed transits for each target $N_{\rm obs,max}$, the slew time between observations $t_{\rm slew}$, ...

double-check which survey params are needed

3.2.1. *Definition of the magma ocean hypothesis and null hypothesis*

Define the null and alternative hypotheses

...

For the likelihood function, we assumed that the planet radii $R_{{\rm P},i}$ are measured with a normally distributed uncertainty $\sigma_{R_{{\rm P},i}}$ and adopted a normal distribution

$$\mathcal{L}(R_{\rm P} \mid \boldsymbol{\theta}) = \prod_i^N \frac{1}{\sqrt{2\pi\sigma^2_{R_{{\rm P},i}}}} \exp\left(-\frac{\left(R_{{\rm P},i} - h\left(\boldsymbol{\theta}, a_{{\rm eff},i}\right)\right)^2}{2\sigma^2_{R_{{\rm P},i}}}\right). \tag{5}$$

Here, $h\left(\boldsymbol{\theta}, a_{{\rm eff},i}\right)$ corresponds to the functional form of the magma ocean hypothesis

link to eqn defining the hypothesis

. We tested this hypothesis against the null hypothesis $h_{\rm null}(\theta, R_{\rm P}) = \theta$, which states that there is no relationship between the measured planet radii and (scaled) semi-major axes.

3.3. *Signature and testability of the magma ocean hypothesis with a $<$ nominaltelescopesize $>$ class space telescope survey*

The fidelity of a future detection or falsification of a magma ocean signature will depend on the significance with which the null hypothesis can be excluded. As a consequence, instrumentation and survey strategy aiming at testing the hypothesis should aim at maximizing the probability of a true positive detection given the existence of the effect. This is called the statistical power of the test. Before turning to mission design trades that influence the statistical power in Sect. 4.4, we explore its behavior as a function of various free parameters of the magma ocean model. ...

3.4. *Statistical power of different mission designs*

show detectability of the magma ocean signature for different mission designs

4. DISCUSSION

4.1. *Implications for planetary habitability*

Magma oceans influence the amount of water available at the surface and atmosphere, which is 1. commonly used as environmental marker to assess habitability, and 2. influences the planet's climate (greenhouse effect).

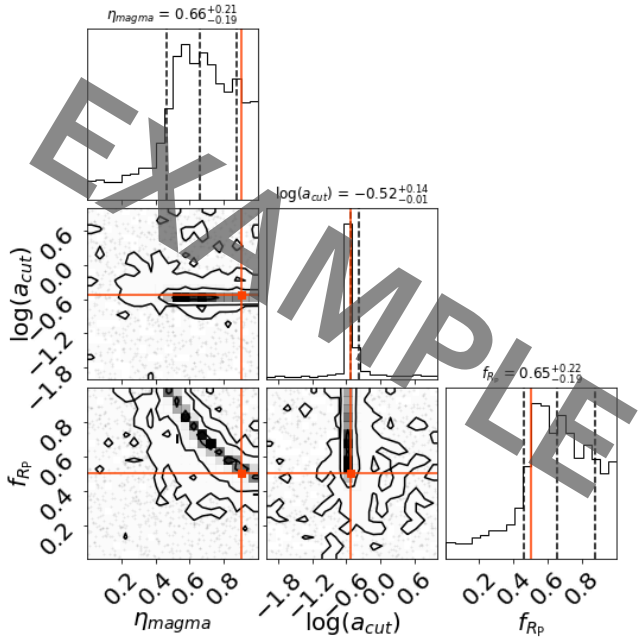

Figure 6. Retrieved posterior distribution of magma ocean model. The density maps in each panel show relationships between and marginalized distributions of the model parameters as they would be retrieved with a targeted < *nominaltelescopesize* > survey of < *surveyduration* > duration. True values of the injected magma ocean parameters are shown in orange. ...

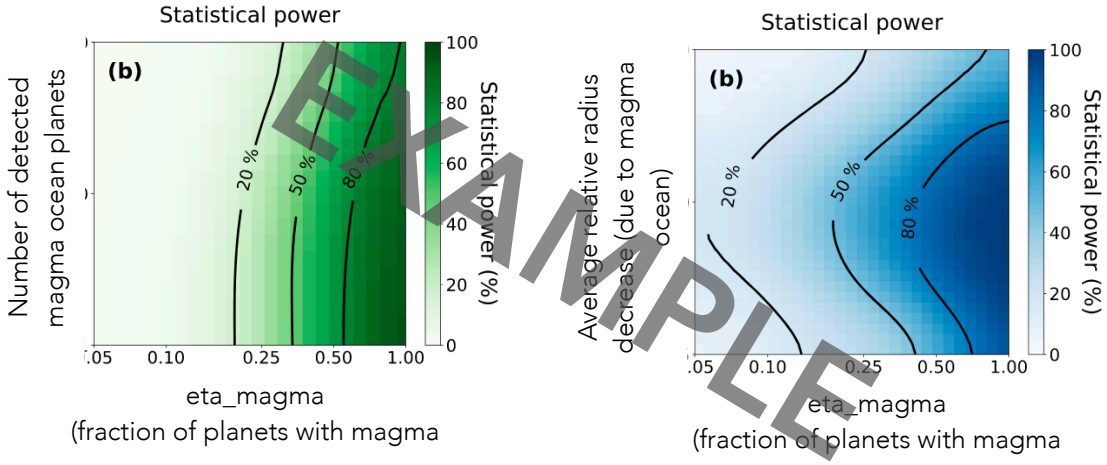

Figure 7. Statistical power of a magma ocean hypothesis test as a function of model parameters.

4.2. *Atmospheric signatures*

discuss potential atmospheric signatures of magma oceans. e.g.: H/O ratios of sub-Neptunes could be low (because H is in the melt) (Tim's talk)

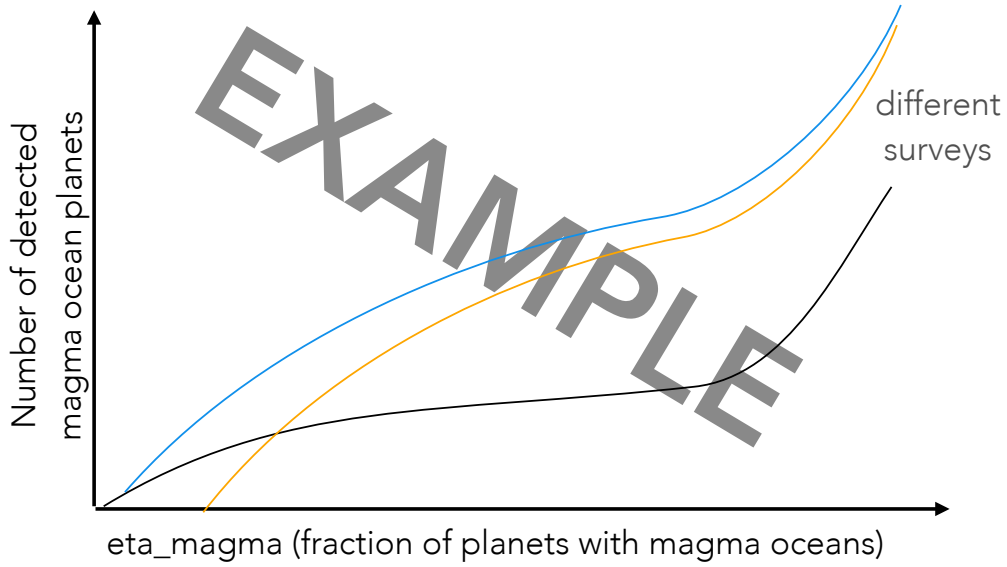

Figure 8. Detections of magma ocean-bearing planets as a function of magma ocean occurrence for different survey designs.

4.3. *False positive scenarios*

what other processes could be confused with a magma ocean signal?

Global magma oceans are not the only physical mechanism that may cause a decrease in transit radii for a subset of planets. Other causes of shrinking planet sizes have been put forward, the most widely discussed ones being atmospheric loss due to either photoevaporation through high-energy radiation by the host star (e.g., Owen & Wu 2013; Jin et al. 2014; Mordasini 2020) or due to residual heat from the planet's interior shortly after formation (Ginzburg et al. 2016, 2018; Gupta & Schlichting 2019). Both processes are being traded as potentially sculpting the observed radius bimodality of small, close-in exoplanets from the *Kepler* mission (Fulton et al. 2017; Van Eylen et al. 2018). Like the magma ocean effect discussed here, these processes reduce the radii of some planets, leading to a decrease in average measured planet radii in a specific region of the planetary parameter space. This region is distinct from the one affected by global magma oceans, since...

...elaborate why they cannot be confused

Another potential false positive contribution comes from the "Neptune desert", a triangular region of low planet occurrence density of close-in planets in period-radius space (Szabó & Kiss 2011; Mazeh et al. 2016; Dreizler et al. 2020). The shape of this region is such that smaller planets become less frequent the closer to the star they are, which to some degree resembles the pattern introduced by the insolation dependency of the magma ocean probability.

explore if this can cause confusion

is there overlap/confusion with the radius/density trend in ??

4.4. *Mission design trades*

Maps to Sect. 3.4.

Penny et al. (2019) mention that a significant increase in planet yield could be achieved if the telescope's slew speed was increased.

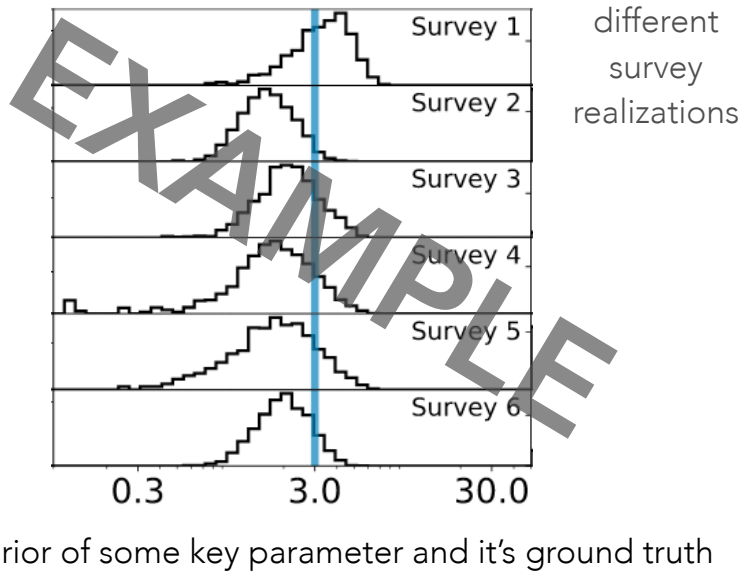

Figure 9. Retrieved posterior distribution of the $< keyparameter >$ for different survey realizations. The orange line corresponds to the true value of the injected signal.

5. CONCLUSIONS

Here or in the introduction: For observations of rocky exoplanets, the currently best-probed regime that of hot, close-in planets. These bodies experience climatic conditions that are similar to the environment of the inner Solar System bodies at early stages of their formation. Studies of the geophysical state and evolution of hot exoplanets can thus contribute to our understanding of the early formation stages of Earth and other habitable worlds.

Author contributions:

Software: Bioverse (Bixel & Apai 2021), Astropy (Astropy Collaboration et al. 2018), NumPy (Harris et al. 2020), SciPy (Virtanen et al. 2020), corner.py (Foreman-Mackey 2016), dynesty (**?**).

REFERENCES

Astropy Collaboration, Price-Whelan, A. M., Sipőcz, B. M., et al. 2018, The Astronomical Journal, 156, 123, doi: 10.3847/1538-3881/aabc4f

Bixel, A., & Apai, D. 2021, The Astronomical Journal, 161, 228, doi: 10.3847/1538-3881/abe042

Dorn, C., & Lichtenberg, T. 2021, The Astrophysical Journal Letters, 922, L4, doi: 10.3847/2041-8213/ac33af

Dreizler, S., I., J., et al. 2020, Astronomy & Astrophysics

Foreman-Mackey, D. 2016, Journal of Open Source Software, 1, 24, doi: 10.21105/joss.00024

Fulton, B. J., Petigura, E. A., Howard, A. W., et al. 2017, The Astronomical Journal, 154, 109, doi: 10.3847/1538-3881/aa80eb

Ginzburg, S., Schlichting, H. E., & Sari, R. 2016, The Astrophysical Journal, 825, 29, doi: 10.3847/0004-637x/825/1/29

—. 2018, Monthly Notices of the Royal Astronomical Society, 476, 759, doi: 10.1093/mnras/sty290

Gupta, A., & Schlichting, H. E. 2019, Monthly Notices of the Royal Astronomical Society, 487, 24, doi: 10.1093/mnras/stz1230

Harris, C. R., Millman, K. J., van der Walt, S. J., et al. 2020, Nature, 585, 357, doi: 10.1038/s41586-020-2649-2

Jin, S., Mordasini, C., Parmentier, V., et al. 2014, Astrophysical Journal, 795, doi: 10.1088/0004-637X/795/1/65

Lichtenberg, T., Schaefer, L. K., Nakajima, M., & Fischer, R. A. 2022, Geophysical Evolution During Rocky Planet Formation

Mazeh, T., Holczer, T., & Faigler, S. 2016, Astronomy and Astrophysics, 589, doi: 10.1051/0004-6361/201528065

Mordasini, C. 2020, Astronomy and Astrophysics, 638, 1, doi: 10.1051/0004-6361/201935541

Owen, J. E., & Wu, Y. 2013, Astrophysical Journal, 775, 1, doi: 10.1088/0004-637X/775/2/105

Penny, M. T., Gaudi, B. S., Kerins, E., et al. 2019, The Astrophysical Journal Supplement Series, 241, 3, doi: 10.3847/1538-4365/aafb69

Schlecker, M., Pham, D., Burn, R., et al. 2021, Astronomy & Astrophysics, 656, A73, doi: 10.1051/0004-6361/202140551

Szabó, G. M., & Kiss, L. L. 2011, Astrophysical Journal Letters, 727, 2, doi: 10.1088/2041-8205/727/2/L44

Van Eylen, V., Agentoft, C., Lundkvist, M. S., et al. 2018, Monthly Notices of the Royal Astronomical Society, 479, 4786, doi: 10.1093/mnras/sty1783

Virtanen, P., Gommers, R., Oliphant, T. E., et al. 2020, Nature Methods, 17, 261, doi: 10.1038/s41592-019-0686-2